Contents lists available at ScienceDirect

Heliyon

journal homepage: www.cell.com/heliyon

Research article

Uridine as a non-toxic actinometer for UV-C treatment: influence of temperature and concentration

Jaayke L. Fiege [a,*], Benedikt Hirt [a], Volker Gräf [a], Stefan Nöbel [b], Dierk Martin [b], Jan Fritsche [b], Katrin Schrader [b], Mario Stahl [a]

[a] Department of Food Technology and Bioprocess Engineering, Max Rubner-Institut, Federal Research Institute of Nutrition and Food, D-76131 Karlsruhe, Germany
[b] Department of Safety and Quality of Milk and Fish Products, Max Rubner-Institut, Federal Research Institute of Nutrition and Food, D-24103 Kiel, Germany

ABSTRACT

UV-C treatment is an effective method to inactivate microorganisms and therefore gets increasingly more attention in food industry, especially for liquid products. To test and monitor different UV-C reactor designs, a photochemical actinometer is required that gives reliable UV-C dose values and is non-toxic allowing frequent control of the production chain. Here, a variable concentrated aqueous uridine solution is tested as a photochemical actinometer. Uridine reacts at 262 nm by photohydration to a single photoproduct not absorbing any light. A concentration dependent quantum yield (Φ) was quantified in the range of 0.2–3.0 mM uridine. Results show that uridine is as accurate as the commonly accepted iodide/iodate actinometry, but not as precise. Especially at higher concentrations a higher number of measurements becomes necessary. Further, a temperature correction is presented for 10 °C > ϑ > 30 °C. Taking these results into account, uridine can certainly be considered as a non-toxic dosimeter for UV-C systems.

1. Introduction

UV-C treatment is of interest in food industry mainly to replace or complement classical pasteurization. Instead of high temperatures, the microorganisms are devitalized by changes in their DNA that cannot be repaired. UV-C energy (approx. 254 nm) leads to the formation of thymine cyclobutene dimers and thus to sterile germs (Beukers and Berends, 1960; Setlow and Setlow, 1962; Swenson and Setlow, 1963). The distinct CO_2 footprint by thermal treatment methods is a strong argument for using low energy consuming UV-C technique in today's food industry (Tran and Farid, 2004; Pennell et al., 2008; Wang et al., 2010; Bandla et al., 2012; Baysal et al., 2013; Flores-Cervantes et al., 2013; Gayán et al., 2013; Groenewald et al., 2013; Cilliers et al., 2014; Ansari et al., 2019). But not just the germicidal effect by UV-C is sensed by the food industry. Current research also focuses on the improvement of certain foods via UV treatment such as vitamin D_3 formation in milk out of its constituents (EFSA, 2016). To avoid partly excessive and/or insufficient treatment of liquid food with UV energy a homogeneous energy distribution is required. Flow-through reactors either need to mix the medium homogeneously using, e.g., turbulent flows, or they need to use laminar flows that are thin enough to allow sufficient penetration of UV-C energy. Especially for turbid or opaque liquids, the latter treatment is challenging. In order to measure the energy input and therefore dose (J/L) that liquid food would experience during treatment in different reactors, an accurate dose measurement is necessary. This is usually done by applying a photometric actinometer. In general, a chemical actinometer utilizes a specific photochemical reaction to determine incident energy dose into a defined volume, which requires exactly known quantum yields (Φ). Quantum yield (Φ) is the number of affected molecules divided by the number of absorbed photons at a specific wavelength (Kuhn et al., 2004; Rabani et al., 2021). The application of chemical actinometric solutions allows the determination of the exact energy release into complex geometries (Kuhn et al., 1989) such as liquids flowing through UV reactors. There are several chemical actinometers published working in the UV-C range (Kuhn et al., 2004; Rabani et al., 2021). However, most actinometers include toxic chemicals or are complicated to use which may work in laboratories but remains challenging for food-producing companies. An easy-to-use and food grade actinometer is required to regularly monitor energy dose values in UV-C food treatment reactors. Therefore, this study focuses on aqueous uridine solution as a chemical actinometer. Uridine is non-toxic as it is one of the unmodified nucleosides usually found in RNA. Uridine contains the chromophore uracil that has an absorption maximum

* Corresponding author.
E-mail addresses: jaayke.fiege@mri.bund.de, jaayke.knipping@web.de (J.L. Fiege).

at approx. 262 nm which, when in aqueous solution, depletes upon UV-C (254 nm) irradiation. This degradation follows (pseudo-) first order kinetics (Wang 1962; von Sonntag and Schuchmann, 1992; Cataldo 2017). The photohydration was identified at the 5–6 double bond at the carbonyl group of the photoproduct (Moore, 1958) that does not absorb any light, neither at 262 nm nor any other wavelength in the UV/Vis range (Figure S1; Moore and Thomson, 1955). This bleaching is even sixteen times more pronounced for the nucleoside uridine when compared to the pure pyrimidine base uracil (Sinsheimer and Hastings, 1949). At neutral pH and 20 °C the photoproduct 6-hydroxy-5,6-dihydrouridine, also called uridine hydrate, is stable for about 150 h (Fisher and Johns, 1976). This, the general availability, low costs (e.g., 200 €/100 g at Carl Roth GmbH, 2022), simple handling (no acids and bases are required), and the non-toxicity of uridine makes it a perfect candidate for a chemical actinometer in food industry using UV-reactor systems. However, the reliability and accuracy of a chemical actinometer are highly dependent on the applied quantum yields. To date, quantum yields are only published for very low uridine concentrations (approx. 10^{-4} Mol/L). At an incident wavelength of 254 nm quantum yields for the photohydration of uridine range between 0.017 and 0.022 Mol/einst (Sinsheimer, 1954; Swenson and Setlow, 1963; Görner, 1991; von Sonntag and Schuchmann, 1992; Gurzadyan and Görner, 1996; Linden and Darby, 1997; Zhang et al., 1997; Jin et al., 2006). While it is generally accepted that the quantum yield of uridine is relatively independent of the incident wavelength, as long as it is in the range of 238–280 nm (Swenson and Setlow, 1963; Rahn and Sellin 1979), the only important factor for uridine degradation relies on the probability whether a photon is or is not absorbed for photohydration (Setlow and Setlow, 1961; Jin et al., 2006). This probability decreases with decreasing incident intensities, i.e. <1 mW/cm² (Linden and Darby, 1997). Additionally, smaller uridine concentrations are said to give more accurate dose values due to Taylor series expansion of the Lambert-Beer law used for calculation of dose values (Jin et al., 2006). However, low concentrated uridine solutions have low absorbances and allow deep UV-C penetration depths into the solution. When penetration depth of the actinometric solution overcomes the width of the treatment space, energy would get lost instead of being measured by the actinometric solution. In order to also measure thin laminar flows a higher uridine concentration becomes necessary when penetration depth is larger than width of the thin film. An actinometric solution with higher uridine concentration would also allow examining large UV doses without falling below the photometric detection limit. However, quantum yields of higher uridine concentration (>10^{-4} Mol/L) were to date not investigated to the best of our knowledge. Thus, quantum yields dependent on higher uridine concentrations (10^{-4} Mol/L< c_{Uridin} < 10^{-2} Mol/L) were investigated in this study as well as compared with standard methods such as iodide/iodate actinometry in different UV-C reactor designs including also a laminar thin film reactor with fluid guiding elements (FGE) generating thin films of 0.06 cm (Gök et al., 2021; Hirt et al. 2022a,b).

2. Material and methods

2.1. Experimental setup

Uridine solutions with variable concentrations were prepared by mixing different masses of uridine (Carl Roth GmbH, Karlsruhe, Germany) into demineralized water. The aimed concentrations were 50, 100, 200, 350, 500 and 750 mg/L, i.e. 0.2, 0.4, 0.8, 1.4, 2.0 and 3.0 mM. In-house built UV-C reactors (Max Rubner-Institut, Karlsruhe, Germany) were used for quantification and validation of the uridine actinometry. All UV-C reactors contain low-pressure mercury lamps with an emission peak at approx. 254 nm. Flow rates for all experiments were adjusted by using a peristaltic pump (Pumpdrive S206; Heidolph Instruments GmbH & Co. KG, Schwabach, Germany) and the uridine solution was pumped five times completely through each reactor. The sample solutions were tempered during the experiments at 20 ± 2 °C (or any other desired temperature) using a coil in a cryostat bath (F32; Julabo GmbH,

Seelbach, Germany). Samples were taken after the preparation of the solution, immediately before UV-C treatment, and after each pass through the reactor. Absorbances after preparation and before UV-C treatment, respectively, remained unchanged proving the stability of the solution to visible light. To prevent mixing with residuals that remained in the reactor from the prior pass, 80 or 200 ml of each pass were discarded before sampling from the coiled tube or straight tube and thin film reactor, respectively. Each uridine concentration was tested in triplicate and each experiment was pumped through the system in five passes generating five data points for each initial concentration. The spread of each data point is given by the standard deviation of n = 3. For comparison exactly the same procedure was conducted for each UV-C reactor type using iodide/iodate actinometry originally developed by Rahn (1997). The iodide (0.6 M) – iodate (0.1 M) solution in 0.01 M borate buffer absorbs all radiation below a wavelength of 290 nm and generates triiodide as a result of a photochemical reaction with UV-C photons (Rahn et al., 2003). Triiodide exhibits an absorbance maximum at 352 nm and its linear formation kinetic allows an easy quantification of absorbed UV-C dose (D in J/L). This actinometric technique is accepted as a standard actinometer (Rabani et al., 2021) and the here reported results are achieved by following the protocols described elsewhere (e.g., Müller et al., 2014, Gök et al., 2021, Hirt et al., 2022a,b).

2.2. UV-C reactors

2.2.1. Coiled tube reactor

This reactor contains a 40 W low-pressure mercury lamp with a specified output of 15 W UV-C (TUV-36-T5; Philips GmbH, Hamburg, Germany) that is surrounded by a 23 m long UV-transparent plastic tube (fluorethylenpropylen: FEP) coiled over a length of 750 mm. The inner tube diameter (d_i) is 3.7 mm and the inner diameter D of the coil is 38.5 mm. Due to centrifugal forces, the medium suppresses liquid from the outer wall so that continuous Dean vortices are generated, when Reynolds numbers (Re) are smaller than the critical Reynolds number (Re_{crit}) and above Dean number values (De) of De_{crit} = 54 (Dean, 1928; Hämmerlin, 1957). This system has a higher critical Reynolds number (Re_{crit}) than simple tube flows with Re_{crit} of approx. 2,300. Re_{crit} in a coiled tube can be calculated using Eq. (1) (Gnielinski, 2010).

$$Re_{crit} = 2300\left[1 + 8.6\left(\frac{d_i}{D}\right)^{0.45}\right] \qquad (1)$$

Re_{crit} of the coiled tube reactor in this study is 9194. The Reynolds number of an aqueous solution in the coiled tube reactor at 30 L/h is calculated using Eq. (2) and accounts for 2868, which is significantly below Re_{crit} of the coiled tube reactor (9,194).

$$Re = \frac{\rho \cdot v \cdot d}{\eta} \qquad (2)$$

v is the velocity (m/s), d is the diameter of the tube (0.0037 m), and ρ is the density (approx. 1,000 kg/m³) and η the dynamic viscosity of the aqueous solution (approx. 1.0 mPa s) at 20 °C. Dean number (De) can be calculated from Re and the inner diameters of the tube (d_i) and the one of the coil (D) (Eq. (3)).

$$De = Re \cdot \sqrt{\frac{d_i}{D}} \qquad (3)$$

The respective Dean number for an aqueous solution at 30 L/h is De = 889, which clearly exceeds De_{crit} = 54. Thus, all experiments at a volume flow of 30 L/h are certainly within the regime of Dean vortices.

2.2.2. Straight tube reactor

The straight tube reactor contains 24 straight tubes having an inner diameter of 6 mm and an outer diameter of 6.6 mm. These tubes consist

of UV-C transparent fluorethylenpropylen (FEP) and are connected with non-UV-transparent U-turns. The total length is 19.3 m of which 16.1 m can be penetrated by the UV light. This tube system is arranged in a commercial UV box (BS04 UV box; UV Messtechnik Opsytec Dr. Gröbel GmbH, Ettlingen, Germany). Twenty 18 W low-pressure mercury lamps with an specified UV-C output of 4.5 W each are positioned 300 mm above the FEP tubes. Thus, the efficiency of the UV lamps is not influenced by the temperature of the medium allowing the investigation of the temperature dependence of the quantum yield. The straight tube reactor can be run at laminar ($Re < 2,300$) and turbulent flow conditions ($Re > 2,300$) by adjusting the flow rate of the medium. Re is calculated in the straight tube systems according to Eq. (2) with diameter d of the straight tube (0.006 m). Hence, when volume flow exceeds 40 L/h, the regime changes from laminar to turbulent flow. Also, the intensity of the UV-C energy of the lamps can be electronically dimmed from 100 to 1 % allowing the investigation of different UV-C intensities independent of the flow rate. The punctual irradiance (mW/cm^2) can be measured with the radiometric sensor included in the commercial UV box (BS04 UV box; UV Messtechnik Opsytec Dr. Gröbel GmbH, Ettlingen, Germany).

2.2.3. Laminar thin film reactor

The core of the thin film reactor (TFR) is a 20 W low-pressure mercury lamp (UVpro N20-2, orca GmbH) with a 7.5 W UV-C output. The medium is pumped with 60 L/h as a laminar thin film of ca. 3.1 mm between the quartz glass cylinder of the lamp and the stainless-steel sleeve over a length of 34.6 cm. To improve the efficiency of UV-C irradiation into opaque liquid foods (e.g. milk) fluid guiding elements (FGE) are inserted into the annular gap (Gök et al., 2021, Hirt et al., 2022a,b). The FGE are made of stainless steel and were designed by the Institute of Micro Process Engineering of the Karlsruhe Institute of Technology (KIT) and manufactured using selective laser melting. These FGE divide the original liquid flow into three partial flows with smaller diameters that are guided alternately towards the UV-C source. Hansjosten et al. (2018) already showed the efficiency of FGE used in pipe-in-pipe heat exchanger wherein the length of the heat exchanger was able to be reduced by ten times. When using FGE in this study the resulting gap between quartz glass and inner wall of the FGE is 0.6 mm, which significantly increases the UV-C efficiency in laminar flowing liquids with high absorbances shown by Gök et al. (2021) and Hirt et al. (2022a,b).

2.3. Photometric measurements

All samples were measured in disposable semi-micro UV cuvettes with an optical path length of 10 mm using a Unicam UV2-100 UV/Vis Spectrometer immediately after irradiation of the samples (<20 min). The absorbance was measured at the maximum of the uridine peak (approx. 262 nm). To achieve reliable results, samples were diluted concerning their initial concentrations to keep maximum absorbances <1.5. Each sample was measured in triplicate (n = 3).

3. Results and discussion

3.1. Quantification of extinction coefficient

To calculate UV doses, the extinction coefficient of the uridine solution is necessary. Since the photoproduct of uridine, uridine hydrate, does not absorb any light the spectrometric detection at solely 262 nm, is sufficient to quantify the photohydration (e.g., Rabani et al., 2021). Photometric scans from 230 to 900 nm of a highly concentrated uridine solution (750 mg/L = 3×10^{-3} Mol/L) before and after UV-C treatment prove that no other light absorbing products were formed (Figure S1). Literature data on extinction coefficients of uridine vary between 8,000 and 10,185 L mol^{-1}·cm^{-1} (von Sonntag and Schuchmann, 1992; Jin et al., 2006; Cataldo 2017). Here, 16 different uridine concentrations ranging between 0.0041 and 500 mmol/L, i.e. 1 and 125,000 mg/L, were measured to determine the extinction coefficient. In order to keep absorbances below 1.5 each

concentration was diluted accordingly and measured in triplicate. The three linear regression slopes gave an average extinction coefficient of 9,560.7 L mol^{-1}·cm^{-1} with a standard deviation of 50.9 L mol^{-1}·cm^{-1} (Figure S2) that fits well within the data published previously (von Sonntag and Schuchmann, 1992; Jin et al., 2006; Cataldo 2017).

3.2. Calculation of actinometric dose (J/L)

This study aimed to develop a chemical actinometer that can be applied independent of the knowledge about the geometry of a reactor and, thus, the total fluence or dosage per 1 L of actinometric solution passing through the reactor ($[D] = J \cdot L^{-1}$) is investigated here instead of spatial and time-resolved irradiance or fluence rate ($[E] = J \cdot cm^{-2} \cdot s^{-1}$). To do so, the equation given by Zhang et al. (1997) was modified similar to the equation given by Rahn (1997) for the potassium iodide actinometer. However, the uridine actinometer follows a reaction of pseudo first-order kinetics (Figure S3 and Wang, 1962; von Sonntag and Schuchmann, 1992; Cataldo, 2017), while the potassium iodide actinometer linearly depends on the formation of triiodide. Thus, the numerator of Eq. (4) needs to be logarithmized in contrast to the potassium iodide equation by Rahn (1997).

$$E \left(\frac{einst}{L} \right) = \frac{ln\left(\frac{A_0}{A_i}\right)}{2.303 \cdot pl \cdot \Phi \cdot \varepsilon_\lambda} \tag{4}$$

A_0 and A_i are the dimensionless absorbances at 262 nm measured before and after treatment through the reactor, respectively, pl is the pathlength of the cuvette (1 cm), Φ is the quantum yield (mol/einst), ε_λ is the molar extinction coefficient (L mol^{-1} cm^{-1}) at irradiation wavelength λ, i.e. here 254 nm. The molar extinction coefficient at 254 nm is approximately 85 % of the molar extinction coefficient measured for 262 nm (Figure S1). To achieve the absolute dosage D (J/L) per pass through the reactor the photon flux P_λ (J/einst) at the irradiation wavelength λ is also required (Eq. (5)):

$$P_\lambda = \frac{h \cdot c}{\lambda} 6.022 \cdot 10^{23} \tag{5}$$

h is the Planck constant (6.626×10^{-34} m^2 kg s^{-1}), c is the speed of light (3×10^8 m s^{-1}) and λ the respective wavelength (254×10^{-9} m). When incident wavelength is 254 nm, P_λ becomes 4.716×10^5 J/einst. Multiplication of P_λ with Eq. (4) results in the absolute dosage D (J/L):

$$D \left(\frac{J}{L} \right) = \frac{ln\left(\frac{A_0}{A_i}\right)}{2.303 \cdot pl \cdot \Phi \cdot \varepsilon_\lambda} \cdot P_\lambda \tag{6}$$

3.3. Concentration dependency of quantum yield Φ

The absorbance A_i changes with each pass through the reactor, while the delivered energy from the UV-C source is constant. Since the remaining parameters are also constants, quantum yield (Φ) is the only parameter that is allowed to change in Eq. (6) by altering concentration. Thus, quantum yield is dependent on uridine concentration. The dose was previously measured using an often applied, but toxic and, therefore, unfeasible chemical actinometer for the food industry - the iodide/iodate actinometry according to Rahn (1997). The iodide/iodate actinometry was proven as a reliable reference that can be used to determine quantum yields of other chemical actinometers (Goldstein and Rabani, 2008; Rabani et al., 2021). Measuring the dose with iodide/iodate at exactly the same conditions (30 L/h, 20 °C) with triplicates à five passes resulted in 856 ± 54 J/L (n = 3) (Figure S4). Using this value as dose D for the coiled tube reactor, Φ for each pass of all experiments was able to be calculated by converting Eq. (6) in terms of Φ. The resulting Φ were plotted versus the concentration that was measured from the absorbance. It is noteworthy that after each pass of each experiment the concentration depletes slightly, which is why each initial concentration resulted in five

separate datapoints (Figure 1). That is, six different initial uridine concentrations resulted in 30 datapoints that can be empirically modeled by a decreasing power function (Eq. 8) with an R^2 of 0.82.

$$\Phi = 0.00006 \cdot c^{-0.555} \tag{7}$$

Using Eq. (7) a quantum yield can be calculated for any concentration (c in Mol/L) between 50 and 750 mg/L urddine. The average of all initial uridine concentrations in the coiled tube reactor resulted in 986 J/L with a standard deviation of ± 82 J/L (Figure 2), where each initial concentration (n = 6) was measured as a triplicate of five passes. This dose is higher than measured with iodide/iodate actinometry (856 $\pm$ 54 J/L; triplicate (n = 3) à five passes) but the discrepance is not significant (p = 0.30) according to ANOVA test. However, the already small quantum yield of uridine decreases even more with increasing concentration when compared to iodide/iodate actinometry with a relatively constant and significantly higher Φ of approximatly 0.73 mol/einst (Rahn, 1997). Thus, propability for uridine hydration may deplete with increasing concentration also affecting the precision of uridine actinomatery at higer concentrationsas it was already observed in the literature (e.g. Jin et al., 2006). An additional reason for the unprecise results gained by high uridine concentration may be the sharper absorption bands in spectrometric measurements, when compared to the rather broader peaks by lower uridine concentrations (Figure S1). Sharper peaks may have more significant deviations due the unpreventable polychromacity when using a light dispersing element with a slit (monochromator). Lower concentrations and thus broader peaks are less susceptible to these random errors caused by minor misadjustments of the monochromator and cause more stable or precise results. However, accuracy seems to remain at higher concentrations. The difference of accuracy and precision is graphically illustrated in the supplementary (Figure S7). That is, the result of many measurements averages in statistically the same value 986 $\pm$ 82 J/L (Figure 2) (p = 0.97). Thus, as long as a sufficient number of measurements is available, high uridine concentrations ($\leq$750 mg/L) are feasible to be applied as a relatively robust and safe actinometer, when toxic actinomteres need to be avoided.

3.4. Validation with different reactor designs

3.4.1. Straight tube reactor (turbulent)

In a straight tube reactor, where medium was treated completely turbulent (volume flow: 100 L/h), i.e. Reynolds number >2300, the
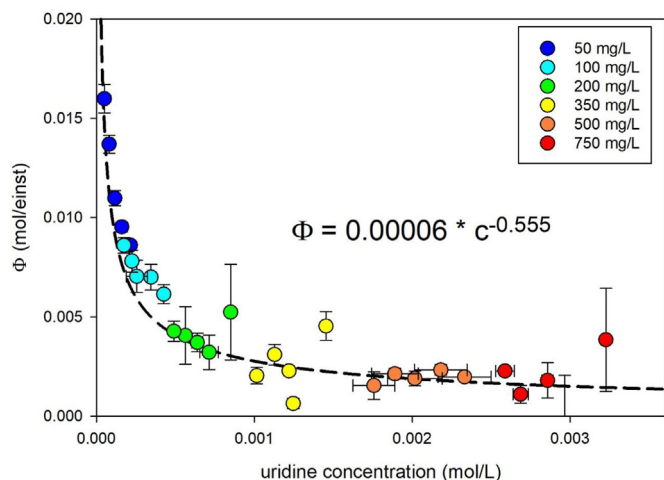

Figure 2. Calculated UV-C dose of six different initial uridine concentrations (Eq. (6), n = 15). Resulting average 986 $\pm$ 82 J/L (n = 6) is displayed (shaded area) as well as averaged UV-C dose measured with iodide/iodate actinometry: 856 $\pm$ 54 J/L (n = 3; dotted area).

absorbances of the different media (iodide/iodate: A_{254nm} = 180 and uridine solution: $30 > A_{254nm} > 2$) should not influence the dose calculation at all. Here, the power of the lamp was varied at 30, 50, 70, and 100%. An initial concentration of 100 mg/L uridine was chosen for different intensities. The dose values using iodide/iodate actinometry after Rahn (1997) (Figure S5) and the ones using uridine actinometry suggested in this work (Eqs. (6) and (7)) were plotted in Figure 3 against the irradiance (mW/cm^2) measured with the stationary radiometric sensor. Iodide/iodate actinometry and uridine actinometry have an overlap with a slope discrepancy of less than 5%. Five measurements à five passes were also conducted with a higher concentration of 500 mg/L uridine at 100% lamp power showing a decreasing certainty, i.e. decreasing precision of uridine actinometry with increasing uridine concentration as shown in Section 3.3. However, accuracy remains, i.e. five measurements à five passes with high uridine concentration (500 mg/L) average in the same dose value as one measurement à five passes with lower uridine concentration (100 mg/L).

3.4.2. Thinfim reactor (laminar)

When working with reactors using laminar flowing thin films, pentration depth of the energy into the actinometric solution becomes of

Figure 1. Quantum yield (Φ) vs. uridine concentration. Φ was calculated for each concentration (n = 3) using Eq. (6) with an assumption of D = 856 $\pm$ 54 J/L (measured with iodide/iodate actinometry; n = 3). The colors of the datapoints indicate each experiment with different initial uridine concentration (750, 500, 350, 200, 100 and 50 mg/L) that deplets upon each pass through the UV-C reactor.
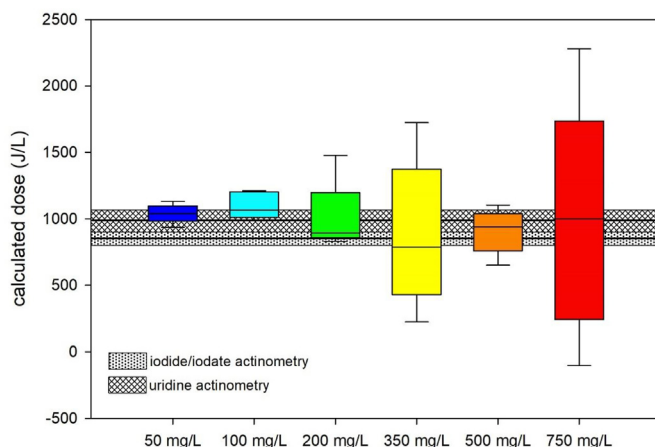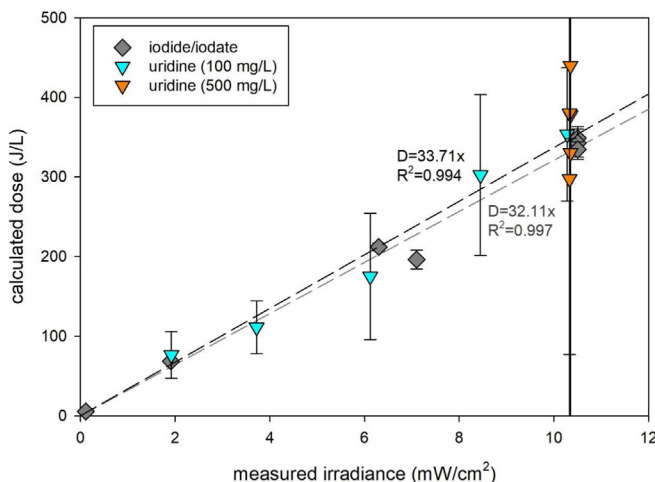

Figure 3. Comparison between iodide/iodate and uridine actinometry in a reactor with turbulent flow (100 L/h) using different incident irradiances. Each data point is based on five passes (n = 5) through the reactor. Uridine concentration was initially 100 or 500 mg/L and quantum yield was calculated according to Eq. (7) in order to calculate the respective dose (Eq. (6)).

high importance, which is in contrast to the previous mentioned reactor designs. The penetration depth (d_p) is the distance at which the intensity of the incoming energy is reduced down to $1/e = 37$ % of the initial energy, as the intensity of an electromagnetic wave decays exponentially inside a medium (Lambert-Beer law). d_p can be calculated from absorbance (A) at according wavelength measured with a photometer (Eq. 8):

$$d_p = \frac{1}{2.303 \cdot A} \qquad (8)$$

The FGE equipped reactor used in this study has a significant smaller treatment width (0.6 mm) than d_p of 254 nm into a 50 mg/L Uridine solution ($d_p = 2.2$ mm) but a larger width than penetration depth into iodide/iodate solution ($d_p = 0.02$ mm). The exponential energy decay for a radial energy source into different uridine concentrations can be calculated using Lambert-Beer law according to Koutchma and Arisi (2004) and Hirt et al. (2022a,b) (Eq. (9)):

$$I_r = I_0 \cdot \frac{r_0}{r} \cdot 10^{-A(r-r_0)} \qquad (9)$$

The results are illustrated in Figure 4 assuming I_0 as 100 % at the outer quartz glass sleeve surrounding the low-pressure mercury lamp ($r_0 = 1.159$ cm) with a maximum penetration depth of 0.063 cm ($r_{max} = 1.222$ cm) (Hirt et al., 2022a,b).

All energy beyond a penetration depth of 0.063 cm, i.e. $r_{max} = 1.222$ cm, is lost to the wall of the FGE and cannot be measured by the actinometric uridine solution. Thus, an "underconcentrated" uridine solution would lead to underestimation of the doses in such laminar thin film system. In order to use uridine solution as reliable chemical actinometer to study/control laminar thin film systems, the uridine concentration needs to be examined at which calculated doses agree with the one of iodide/iodate actinometry. The doses at a volume flow adjusted to 60 L/h were measured with different uridine concentrations as well as with iodide/iodate actinometry resulting in 329 ± 3 J/L for the latter (Figure S6). Each uridine concentration was measured in triplicates à five passes. The results are displayed in Figure 5 together with the theoretical measurable doses from Eq. (9) with $r_0 = 1.159$ cm and $r = 1.222$ cm. It is obvious that actinometric solutions with low uridine concentrations (here <500 mg/L) would significantly underestimate the actual doses applied to the passing medium in this reactor. Thus, higher uridine concentrations are necessary to measure actinometric dose more accurately in laminar thin film systems, although precision depletes with higher concentrations. The required uridine concentration to achieve
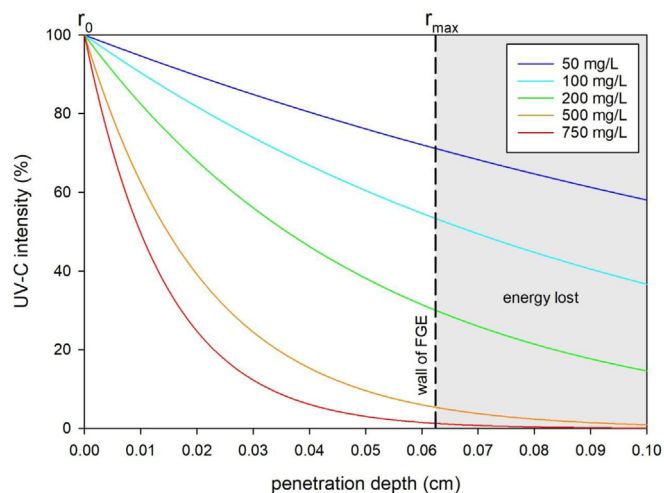

Figure 5. Calculated uridine dose (n = 3) vs. uridine concentration in a thin film reactor equipped with fluid guiding elements (FGE) generating a 0.6 mm laminar thin film passing the UV-C lamp. Laminar volume flow was adjusted to 60 L/h for uridine and iodide/iodate (329 ± 3 J/L) measurements. Theoretical energy loss to the FGE wall is shown as exponential decay towards decreasing uridine concentration (dashed line) with iodide/iodate doses (329 ± 3 J/L) assumed as 100 % energy input.

reliable results depends on the width of the treatment space. Here, a concentration of ≥ 500 mg/L is necessary to achieve similar results as with iodide/iodate actinometry.

3.5. Temperature effect on quantum yield

The effect of the temperature of the medium on the quantum yield was invastigated on the straight tube reactor, where the UV-C lamps are relatively far away from the treated medium (300 mm) and thus are not influenced by the temperature of the treated medium. Uridine actinometry was conducted in triplicates à five passes with 500 mg/L and a turbulent volume flow of 100 L/h. Temperatures were adjusted to three different values (approx. 10, 20, and 30 °C). These temperatures are plotted against the resulting doses from uridine actinometry using Eqs. (6) and (7) in Figure 6. In addition, the dose from iodide/iodate actinometry (342 ± 7 J/L; n = 3) was measured under the same conditions. Since, the calculation by iodide/iodate actinometry already includes a

Figure 4. Exponential decay of UV-C intensity vs. penetration depth into different concentrated actinometric uridine solutions. Distance of FGE wall (0.063 cm) from energy source is displayed as dahed line. All energy beyond this distance is lost for actinometric measurements.
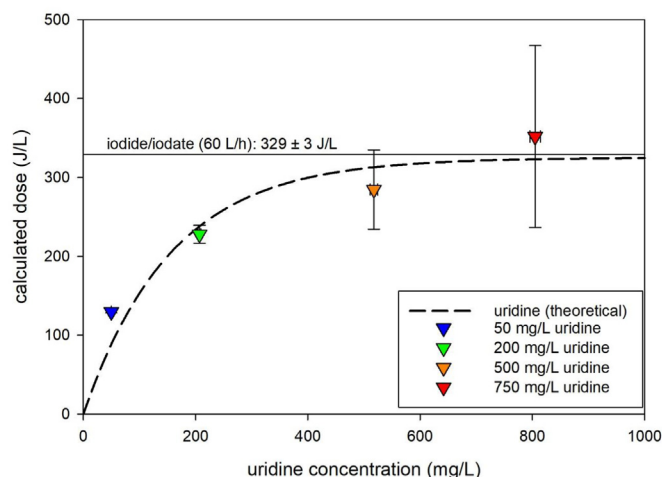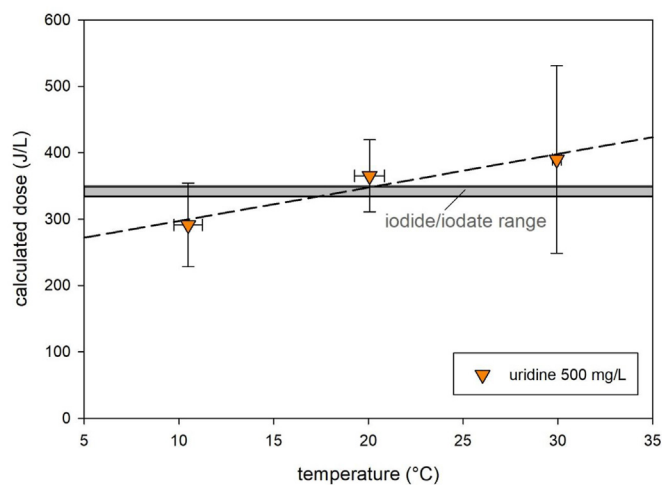

Figure 6. Calculated dose (n = 3) vs. temperature from uridine actinometry (500 mg/L). The iodide/iodate range (gray area) is shown as reference over the whole temperature range since the dose calculation by Rahn (1997) includes a temperature correction.

temperature correction (Rahn, 1997), the iodide/iodate data measured at $19.3 \pm 0.3\ °C$ is plotted as a constant. A positive linear relationship to temperature becomes visible for uridine actinometry. Thus, the measured dose using Eqs. (6) and (7) can be corrected for the applied temperature using the empirical Eq. (10):

$$D_{corr} = D_{meas} - 5\ \frac{J}{L\ °C} \cdot \vartheta + 100\ J \Big/ L \qquad (10)$$

D_{meas} is the measured dose as calculated from Eqs. (6) and (7) in J/L, ϑ is the experimental temperature in $°C$, and D_{corr} is the temperature corrected dose in J/L. This correction stays valid in the range of 10–30 $°C$ and for UV-C reactors where lamp power remains unaffected of the temperature of the treated medium. When UV-C lamps are more proximate to the treated medium, an additional influence of temperature on efficiency of UV-C lamp may arise.

4. Conclusion

If a food-grade actinometric system is required uridine actinometry can be applied as an alternative to the toxic iodide/iodate actinometric system. The results of this study show that concentration of uridine can be varied from 0.2 to 3.0 mM using the here presented concentration dependency for the calculation of the quantum yield ($\Phi = 0.00006*c^{-0.555}$; c in Mol /L). This novel application with also higher concentration (i) extends the total detectable UV-C dosage range and (ii) enables measurements in laminar thin film reactor designs, where width of treatment space is <2.2 mm, which is the penetration depth (d_p) of 254 nm into a commonly concentrated actinometric uridine solution (approx. 0.2 mM uridine). However, as quantum yield decreases with increasing uridine concentration the precision of uridine actinometetry also depletes. Thus, concentration of uridine should be kept as low as possible in order to receive more precise results with low standard deviations. But when concentration needs to be increased e.g. due to the above mentioned reasons, one could simply increase the number of measurements, which is cheap and easy due to low costs and non-toxic behavior of uridine. The results may be not as precise as measured with low concentrated uridine solutions or with iodide/iodate actinometry, but the accuracy remains, i.e. th average of many measurements shall be statistically the same. Additionally, experimental temperature seems to influence the measured dose by uridine actinometry, but measured dose results can be corrected accordingly (10–30 $°C$): $D_{corr} = D_{meas} - 5\ \frac{J}{L°C} \cdot \vartheta(°C) + 100\ J / L$.

Declarations

Author contribution statement

Jaayke L. Fiege: Conceived and designed the experiments; Performed the experiments; Analyzed and interpreted the data; Wrote the paper.

Benedikt Hirt; Volker Gräf; Dierk Martin; Katrin Schrader: Conceived and designed the experiments; Analyzed and interpreted the data; Wrote the paper.

Stefan Nöbel: Conceived and designed the experiments; Wrote the paper.

Jan Fritsche: Analyzed and interpreted the data; Wrote the paper.

Mario Stahl: Contributed reagents, materials, analysis tools or data; Wrote the paper.

Funding statement

Data availability statement

Data included in article/supp. material/referenced in article.

Declaration of interest's statement

The authors declare no conflict of interest.

Additional information

Supplementary content related to this article has been published online at https://doi.org/10.1016/j.heliyon.2022.e11437.

Acknowledgements

References

Ansari, J.A., Ismail, M., Farid, M., 2019. Investigate the efficacy of UV pretreatment on thermal inactivation of Bacillus subtilis spores in different types of milk. Innovat. Food Sci. Emerg. Technol. 52, 387–393.

Bandla, S., Choudhary, R., Watson, D.G., Haddock, J., 2012. UV-C treatment of soymilk in coiled tube UV reactors for inactivation of Escherichia coli W1485 and Bacillus cereus endospores. LWT–Food Sci. Technol. 46 (1), 71–76.

Baysal, A.H., Molva, C., Unluturk, S., 2013. UV-C light inactivation and modeling kinetics of Alicyclobacillus acidoterrestris spores in white grape and apple juices. Int. J. Food Microbiol. 166 (3), 494–498.

Beukers, R., Berends, W., 1960. Isolation and identification of the irradiation product of thymine. Biochim Biophys Acta 41, 550–551.

Cataldo, F.S., 2017. Uridine as photochemical actinometer: application to LED-UV flow reactors. Eur. Chem. Bull. 6 (9), 405–409.

Cilliers, F.P., Gouws, P.A., Koutchma, T., Engelbrecht, Y., Adriaanse, C., Swart, P., 2014. A microbiological, biochemical and sensory characterisation of bovine milk treated by heat and ultraviolet (UV) light for manufacturing Cheddar cheese. Innovat. Food Sci. Emerg. Technol. 23, 94–106.

Dean, W.R., 1928. Fluid motion in a curved channel. Proc. R. Soc. Lond. – Ser. A Contain. Pap. a Math. Phys. Character 121 (787), 402–420.

EFSA Panel on Dietetic Products, Nutrition and Allergies (NDA), 2016. Safety of UV-treated milk as a novel food pursuant to Regulation (EC) No 258/97. EFSA J. 14 (1), 4370.

Fisher, G.J., Johns, H.E., 1976. In: Wang, S.Y. (Ed.), Photochemistry and Photobiology of Nucleic Acids, 1. Academic Press, New York, p. 169.

Flores-Cervantes, D., Palou, E., López-Malo, A., 2013. Efficacy of individual and combined UVC light and food antimicrobial treatments to inactivate Aspergillus flavus or A. Niger spores in peach nectar. Innovat. Food Sci. Emerg. Technol. 20, 244–252.

Gayán, E., Álvarez, I., Condón, S., 2013. Inactivation of bacterial spores by UV-C light. Innovat. Food Sci. Emerg. Technol. 19, 140–145.

Gnielinski, V., 2010. Heat transfer in helically coiled tubes. In: VDI (Ed.), Heat Atlas, second ed. Springer, Berlin, p. 709.

Gök, S.B., Vetter, E., Kromm, L., Hansjosten, E., Hensel, A., Gräf, V., Stahl, M., 2021a. Inactivation of E. coli and L. innocua in milk by a thin film UV-C reactor modified with flow guiding elements (FGE). Int. J. Food Microbiol. 343, 109-105.

Goldstein, S., Rabani, J., 2008. The ferrioxalate and iodide–iodate actinometers in the UV region. J. Photochem. Photobiol. Chem. 193 (1), 50–55.

Görner, H., 1991. Chromophore loss of uracil derivatives and polyuridylic acid in aqueous solution caused by 248 nm laser pulses and continuous UV irradiation: mechanism of the photohydration of pyrimidines. J. Photochem. Photobiol. B Biol. 10 (1-2), 91–110.

Groenewald, W., Gouws, P., Cilliers, F., Witthuhn, R., 2013. The use of ultraviolet radiation as a non-thermal treatment for the inactivation of Alicyclobacillus acidoterrestris spores in water, wash water from a fruit processing plant and grape juice concentrate. J. New Gener. Sci. 11 (2), 19–32.

Gurzadyan, G.G., Görner, H., 1996. Depopulation of highly excited singlet states of DNA model compounds: quantum yields of 193 and 245 nm photoproducts of pyrimidine monomers and dinucleoside monophosphates. Photochem. Photobiol. 63 (2), 143–153.

Hämmerlin, G., 1957. Die Stabilität der Strömung in einem gekrümmten Kanal. Arch. Ration. Mech. Anal. 1 (1), 212–224.

Hansjosten, E., Wenka, A., Hensel, A., Benzinger, W., Klumpp, M., Dittmeyer, R., 2018. Custom-designed 3D-printed metallic fluid guiding elements for enhanced heat transfer at low pressure drop. Chem. Eng. Process. – Process Intensification 130, 119–126.

Hirt, B., Hansjosten, E., Hensel, A., Gräf, V., Stahl, M., 2022a. Improvement of an annular thin film UV-C reactor by fluid guiding elements. Innovat. Food Sci. Emerg. Technol. 77, 102988.

Hirt, B., Fiege, J., Cvetkova, S., Gräf, V., Scharfenberger-Schmeer, M., Durner, D., Stahl, M., 2022b. Comparison and prediction of UV-C inactivation kinetics of S. cerevisiae in model wine systems dependent on flow type and absorbance. LWT–Food Sci. Technol. 169, 114062.

Jin, S., Mofidi, A.A., Linden, K.G., 2006. Polychromatic UV fluence measurement using chemical actinometry, biodosimetry, and mathematical techniques. J. Environ. Eng. 132 (8), 831–841.

Koutchma, T., Arisi, B.P., 2004. Biodosimetry of Escherichia coli UV inactivation in model juices with regard to dose distribution in annular UV reactors. J. Food Sci. 69 (1), FEP14–FEP22.

Kuhn, H.J., Braslavsky, S.E., Schmidt, R., 1989. Chemical actinometry. Pure Appl. Chem. 61 (2), 187–210.

Kuhn, H.J., Braslavsky, S.E., Schmidt, R., 2004. Chemical actinometry (IUPAC technical report). Pure Appl. Chem. 76 (12), 2105–2146.

Linden, K.G., Darby, J.L., 1997. Estimating effective germicidal dose from medium pressure UV lamps. J. Environ. Eng. 123 (11), 1142–1149.

Moore, A.M., Thomson, C.H., 1955. Ultraviolet irradiation of pyrimidine derivatives. Science 122 (3170), 594–595.

Moore, A.M., 1958. Ultraviolet irradiance of pyrimidine derivatives II. Note on the synthesis of the product of reversible photolysis of uracil. Can. J. Chem. 36 (1), 281–283.

Müller, A., Stahl, M.R., Greiner, R., Posten, C., 2014. Performance and dose validation of a coiled tube UV-C reactor for inactivation of microorganisms in absorbing liquids. J. Food Eng. 138, 45–52.

Pennell, K.G., Naunovic, Z., Blatchley III, E.R., 2008. Sequential inactivation of bacillus subtilis spores with ultraviolet radiation and iodine. J. Environ. Eng. 134 (7), 513–520.

Rahn, R.O., Sellin, H.G., 1979. Quantum yield of photohydration for dimethyluracil. Concentration and wavelength dependence. Photochem. Photobiol. 30 (2), 317–318.

Rahn, R.O., 1997. Potassium iodide as a chemical actinometer for 254 nm radiation: use of Iodate as an electron scavenger. Photochem. Photobiol. 66 (4), 450–455.

Rabani, J., Mamane, H., Pousty, D., Bolton, J.R., 2021. Invited review practical chemical actinometry—a review. Photochem. Photobiol. 97, 873–902.

Setlow, R.B., Setlow, J.K., 1962. Evidence that ultravioletinduced thymine dimers in DNA cause biological damage. Proc. Natl. Acad. Sci. U. S. A. 48 (7), 1250.

Sinsheimer, R.L., Hastings, R., 1949. A reversible photochemical alteration of uracil and uridine. Science 110 (2864), 525–526.

Sinsheimer, R.L., 1954. The photochemistry of uridylic acid. Radiat. Res. 1 (6), 505 513.

Swenson, P.A., Setlow, R.B., 1963. Kinetics of dimer formation and photohydration in ultraviolet-irradiated polyuridylic acid. Photochem. Photobiol. 2 (4), 419–434.

Tran, M.T.T., Farid, M., 2004. Ultraviolet treatment of orange juice. Innovat. Food Sci. Emerg. Technol. 5 (4), 495–502.

von Sonntag, C., Schuchmann, H.P., 1992. UV disinfection of drinking water and by product formation - some basic considerations. J. Water Supply Res. Technol. – Aqua 41 (2), 67–74.

Wang, S.Y., 1962. Analysis of the rate of the ultraviolet irradiation and reconstitution reactions of 1,3-dimethyluracil and uridine. Photochem. Photobiol. 1 (2), 135–145.

Wang, D., Oppenländer, T., El-Din, M.G., Bolton, J.R., 2010. Comparison of the disinfection effects of vacuum-UV (VUV) and UV light on Bacillus subtilis spores in aqueous suspensions at 172, 222 and 254 nm. Photochem. Photobiol. 86 (1), 176–181.

Zhang, J.Y., Boyd, I.W., Esrom, H., 1997. UV intensity measurement for a novel 222 nm excimer lamp using chemical actinometer. Appl. Surf. Sci. 109, 482–486.